



Site-selective Assembly between 1,8-Diodoperfluorooctane and 4,7,8,11-Tetraazahelicene driven by Halogen Bonding

Serena Biella, Massimo Cametti, Tullio Caronna, Gabriella Cavallo,
Alessandra Forni, Pierangelo Metrangolo, Tullio Pilati, Giuseppe Resnati,
Giancarlo Terraneo

► To cite this version:

Serena Biella, Massimo Cametti, Tullio Caronna, Gabriella Cavallo, Alessandra Forni, et al.. Site-selective Assembly between 1,8-Diodoperfluorooctane and 4,7,8,11-Tetraazahelicene driven by Halogen Bonding. *Supramolecular Chemistry*, 2011, 23 (03-04), pp.256-262. 10.1080/10610278.2010.521841 . hal-00687342

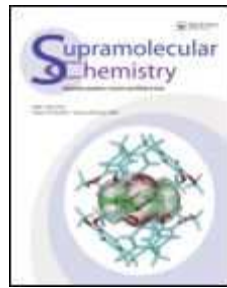
HAL Id: hal-00687342

<https://hal.science/hal-00687342>

Submitted on 13 Apr 2012

HAL is a multi-disciplinary open access archive for the deposit and dissemination of scientific research documents, whether they are published or not. The documents may come from teaching and research institutions in France or abroad, or from public or private research centers.

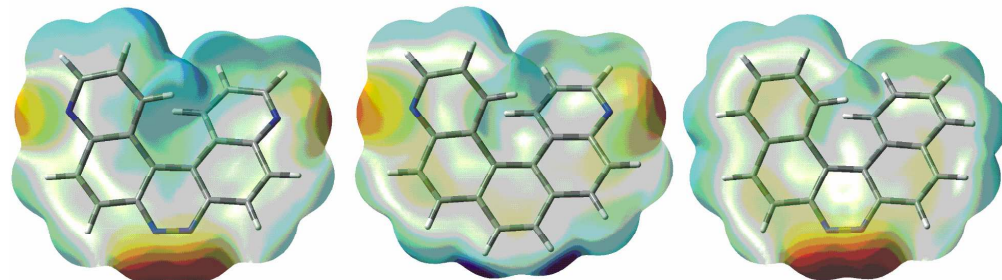
L'archive ouverte pluridisciplinaire **HAL**, est destinée au dépôt et à la diffusion de documents scientifiques de niveau recherche, publiés ou non, émanant des établissements d'enseignement et de recherche français ou étrangers, des laboratoires publics ou privés.



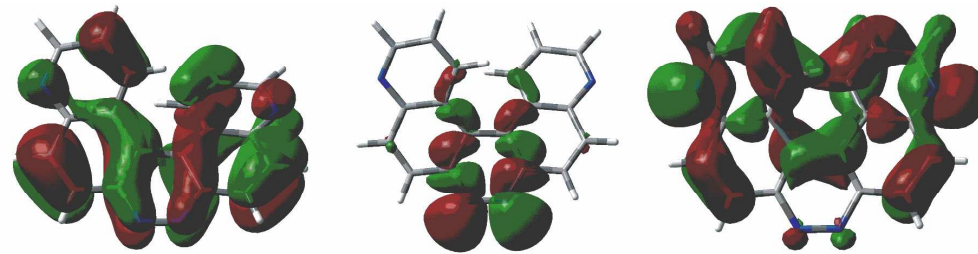
Site-selective Assembly between 1,8-Diiodoperfluorooctane and 4,7,8,11-Tetraazahelicene driven by Halogen Bonding

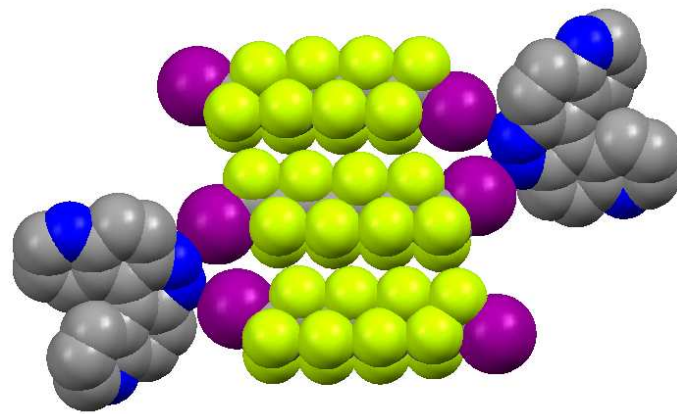
Journal:	<i>Supramolecular Chemistry</i>
Manuscript ID:	GSCH-2010-0168.R1
Manuscript Type:	Special Issue Paper
Date Submitted by the Author:	20-Aug-2010
Complete List of Authors:	Biella, Serena; Politecnico di Milano Cametti, Massimo; Politecnico di Milano Caronna, Tullio; Università di Bergamo Cavallo, Gabriella; Politecnico di Milano Forni, Alessandra; ISTM-CNR Metrangolo, Pierangelo; Politecnico di Milano Pilati, Tullio; ISTM-CNR Resnati, Giuseppe; Politecnico di Milano Terraneo, Giancarlo; Politecnico di Milano
Keywords:	halogen bonding, diiodoperfluoroalkanes, azahelicenes, X-ray structure, DFT studies
Note: The following files were submitted by the author for peer review, but cannot be converted to PDF. You must view these files (e.g. movies) online.	
Scheme 1.cdx Scheme 1_BW.cdx	

SCHOLARONE™
Manuscripts

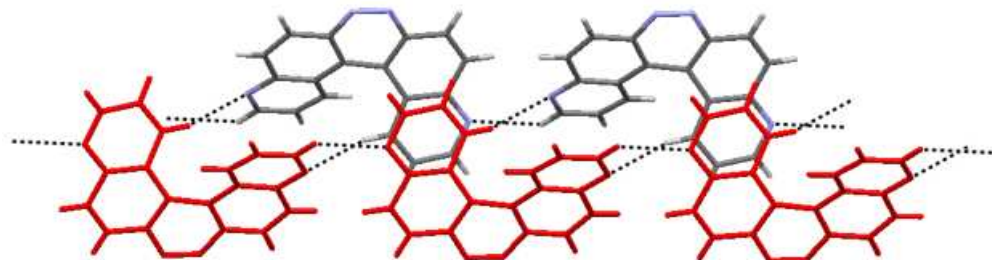


or Peer Review Only

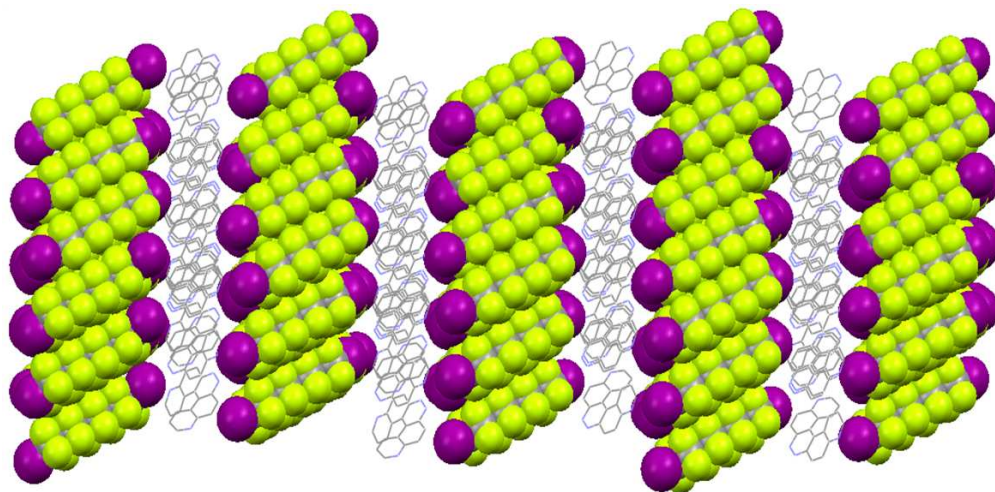




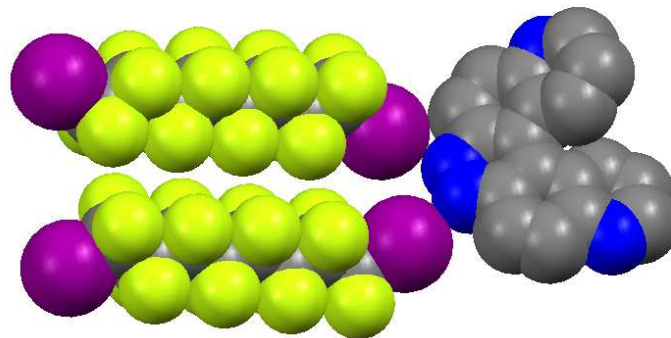
359x155mm (72 x 72 DPI)



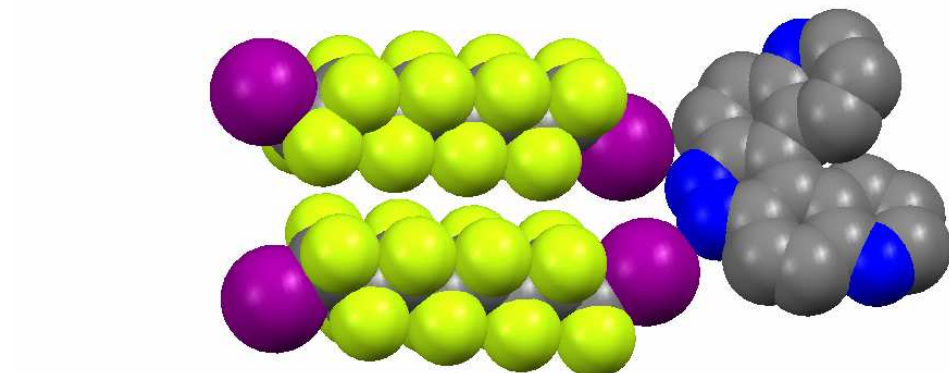
165x56mm (96 x 96 DPI)



233x103mm (127 x 142 DPI)



359x155mm (72 x 72 DPI)

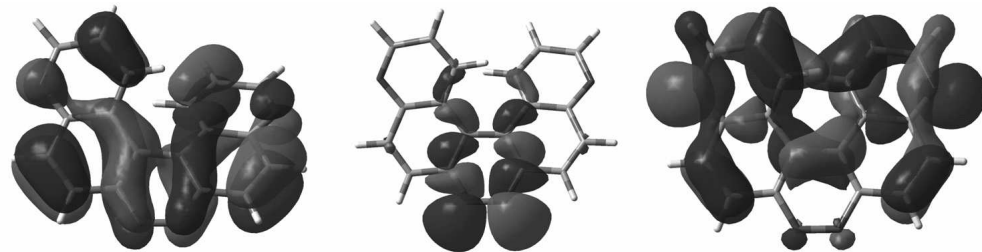


The self-assembly of 1,8-diiodoperfluorooctane with 4,7,8,11-tetraazahelicene revealed a site-selective pattern of halogen bonds in the solid state. In fact, the N···I-C bonding formation occurred selectively on the pyridazinic/cinnolinic nitrogen atoms of the tetraazahelicene unit, which were preferred over the pyridinic/quinolinic ones. DFT calculations predicted and explained well this site-selective halogen bonding formation.



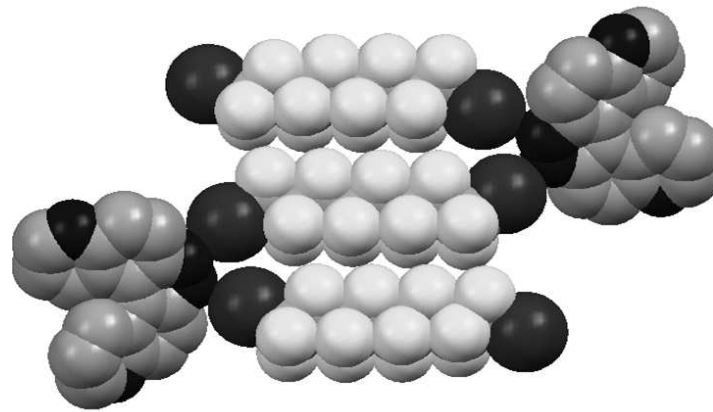
254x74mm (150 x 150 DPI)

Peer Review Only



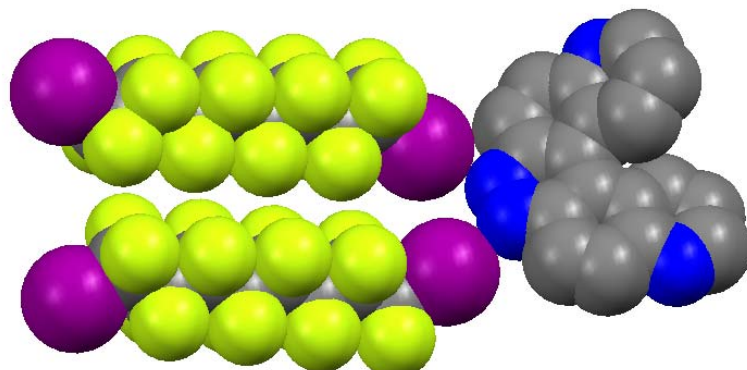
254x64mm (150 x 150 DPI)

Peer Review Only

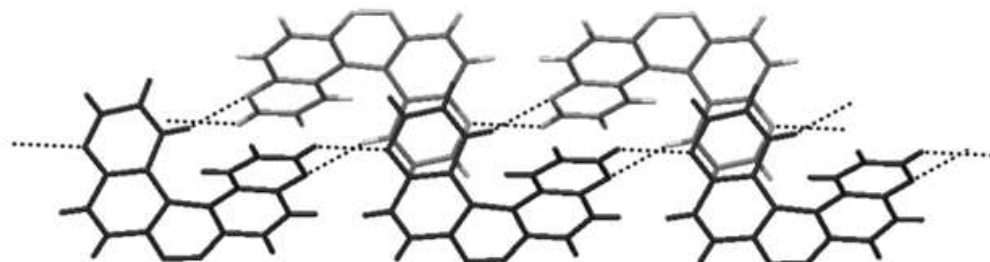


254x116mm (102 x 96 DPI)

1
2
3
4
5
6
7
8
9
10
11
12
13
14
15
16
17
18
19
20
21
22
23
24
25
26
27
28
29
30
31
32
33
34
35
36
37
38
39
40
41
42
43
44
45
46
47
48
49
50
51
52
53
54
55
56
57
58
59
60

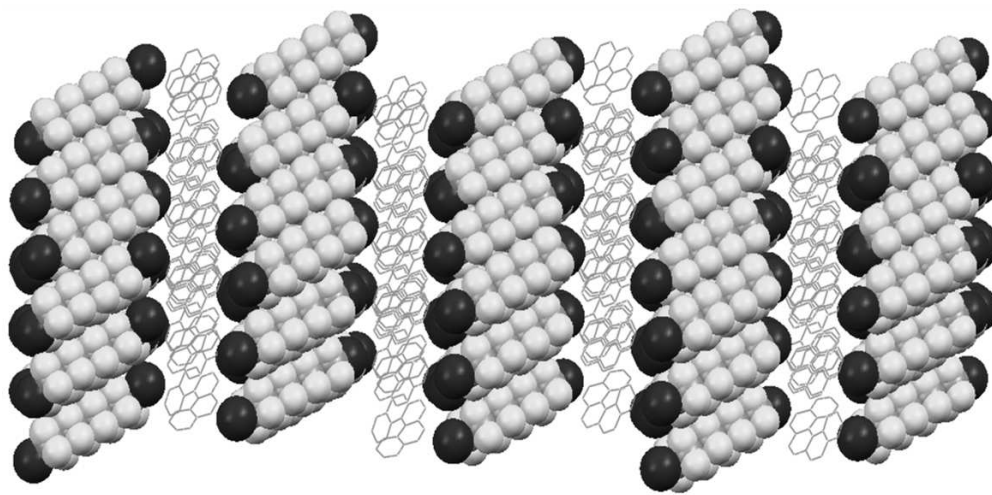


The self-assembly of 1,8-diiodoperfluorooctane with 4,7,8,11-tetraazahelicene revealed a site-selective pattern of halogen bonds in the solid state. In fact, the N···I-C bonding formation occurred selectively on the pyridazinic/cinnolinic nitrogen atoms of the tetraazahelicene unit, which were preferred over the pyridinic/quinolinic ones. DFT calculations predicted and explained well this site-selective halogen bonding formation.



254x86mm (62 x 62 DPI)

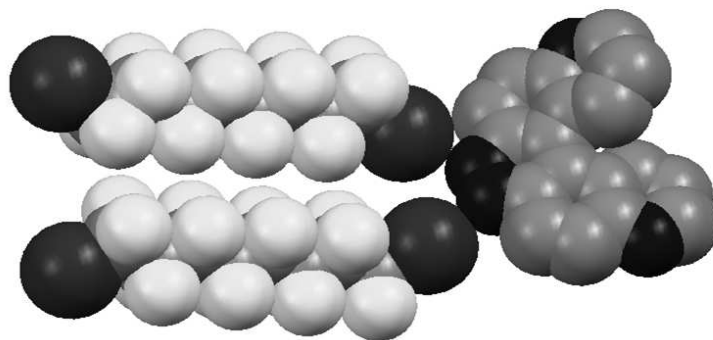
Peer Review Only



233x103mm (127 x 142 DPI)

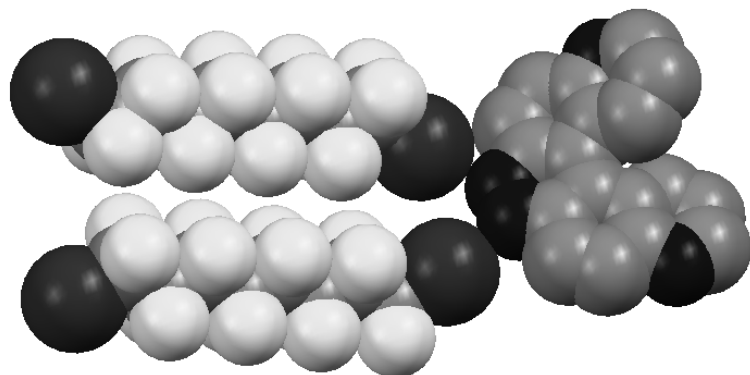
Review Only

1
2
3
4
5
6
7
8
9
10
11
12
13
14
15
16
17
18
19
20
21
22
23
24
25
26
27
28
29
30
31
32
33
34
35
36
37
38
39
40
41
42
43
44
45
46
47
48
49
50
51
52
53
54
55
56
57
58
59
60



254x116mm (102 x 96 DPI)

1
2
3
4
5
6
7
8
9
10
11
12
13
14
15
16
17
18
19
20
21
22
23
24
25
26
27
28
29
30
31
32
33
34
35
36
37
38
39
40
41
42
43
44
45
46
47
48
49
50
51
52
53
54
55
56
57
58
59
60



The self-assembly of 1,8-diiodoperfluorooctane with 4,7,8,11-tetraazahelicene revealed a site-selective pattern of halogen bonds in the solid state. In fact, the N···I-C bonding formation occurred selectively on the pyridazinic/cinnolinic nitrogen atoms of the tetraazahelicene unit, which were preferred over the pyridinic/quinolinic ones. DFT calculations predicted and explained well this site-selective halogen bonding formation.

Site-selective Assembly between 1,8-Diodoperfluorooctane and 4,7,8,11-Tetraazahelicene driven by Halogen Bonding

Serena Biella^{a,b}; Massimo Cametti^a; Tullio Caronna^c; Gabriella Cavallo^{a,b};
Alessandra Forni^d; Pierangelo Metrangolo^{a,b,*}; Tullio Pilati^d; Giuseppe
Resnati^{a,b,d,*}; Giancarlo Terraneo^{a,b}

^aNFMLab, DCMIC “Giulio Natta”, Politecnico di Milano, via Mancinelli 7, I-20131
Milan (Italy); ^bCNST-IIT@POLIMI, Politecnico di Milano, via Pascoli 70/3, I-20133
Milan (Italy); ^cDipartimento di Ingegneria industriale, Università di Bergamo, viale
Marconi 5 - 24044 Dalmine (BG, Italy); ^dInstitute of Molecular Science and
Technology, CNR – University of Milan, via Golgi 19, I-20133 Milan (Italy)

*Corresponding authors. Email: pierangelo.metrangolo@polimi.it;
giuseppe.resnati@polimi.it

(Received XX Month Year; final version received XX Month Year)

The X-ray diffraction analysis on single crystals obtained from the self-assembly of 1,8-diodoperfluorooctane **1** with the tetraazahelicene derivative **2** revealed a site-selective pattern of halogen bonds (XBs) in the solid state. Indeed, two non-equivalent halogen bonds drive the formation of an indefinitely repeating pentameric **(1)₃(2)₂** unit. Interestingly, the N···I-C bonding formation occurred selectively on the pyridazinic/cinnolinic nitrogen atoms of the tetraazahelicene unit, which were preferred over the pyridinic/quinolinic ones. On the basis of MEP and MO analyses, DFT calculations predicted and explained well this site-selective XB formation, thus demonstrating to be efficient tools for the prediction of the XB site-selectivity in similar polynitrogen systems.

Deleted: bondings

Deleted: bondings

Keywords: halogen bonding; diiodoperfluoroalkanes, azahelicenes, X-Ray structure, DFT studies, Molecular Electronic Potential (MEP), Molecular Orbital (MO).

1. Introduction

The search for materials endowed with novel properties is strategic for the development of technological applications, yet extremely challenging (1). One of the leading approaches to obtain new materials is self-assembly, which consists of the design of a set of components, *i.e.* molecular building blocks, which, assemble each to the other in a controlled fashion due to their intrinsic structural and electronic properties (2). In order to achieve control over the desired architecture, non-covalent interactions, a broad category which encompasses forces of various nature, are used for gluing the molecular building blocks together. For this reason, non-covalent interactions are subjected to meticulous and continuous investigation by the scientific community (3). In fact, the precise understanding of such interactions is a

fundamental prerequisite for the design of functional building blocks and for their full exploitation in materials chemistry.

The polarization effect exerted by strong electron-withdrawing groups renders a nearby halogen atom an excellent acceptor of electron density from an electron-rich donor. Such a type of interaction, disregarded only a few years ago, has been recently rediscovered and the term *halogen bonding* (4) has been introduced for describing any noncovalent interaction involving the positive region of the electrostatic potential surface of halogen atoms (5). The general scheme D···X-Y thus applies to halogen bonding (XB), wherein X is the halogen (Lewis acid, XB-donor), D is any electron-donor (Lewis base, XB-acceptor), and Y is carbon, halogen, nitrogen, etc. The term *halogen bonding* itself sheds light on the nature of XB, which possesses numerous similarities with hydrogen bonding (HB), wherein hydrogen functions as the acceptor of electron density.

In the last decade or so, XBs have been thoroughly investigated in order to acquire insight on the physical determinants that cement together XB-donors and acceptors (6). Generally, XB is considered to rely on a dominant electrostatic term, but other contributions are certainly present spanning from polarization and dispersion forces to charge-transfer interactions. The iodine atom, given its lower electronegativity and larger polarizability in the halogen series, performs best as a XB-donor, provided that strong electron-withdrawing groups are present in close proximity with the halogen atom.

Scheme 1

Among the various classes of molecules that can interact via XB, linear mono- and bis-iodo-perfluoroalkanes, *i.e.* the 1,8-diiodoperfluoroalkane **1** (Scheme 1), are among the most commonly employed XB-donors (7). Perfluorocarbon residues are strongly electron-withdrawing, and in addition, the -(CF₂)_n- chain in a perfluoroalkane is significantly more stiff than the -(CH₂)_n- chain in its hydrocarbon analogue and this confers an extra advantage in terms of preorganization and structural control.

On the other hand, aromatic and aliphatic nitrogen-containing rings and their N-oxide derivatives function as XB-acceptors and have been effectively employed as building blocks for the self-assembly of various X-bonded supramolecular architectures (4). However, little is known on how to control selectivity among

different electron-donor sites in polynitrogen-containing heterocyclic systems. Recently we reported an interesting case of site-selective supramolecular synthesis in X-bonded systems, wherein only the pyridinic nitrogen atoms of trans-4,4'-azobipyridine were involved in the recognition process (8). In order to increase the number of cases of site-selective XB-formation in polynitrogen systems, we decided to undertake the study of the XB-acceptor behaviour of the tetraazahelicene derivative **2**, which presents both pyridinic/quinolinic and pyridazinic/cinnolinic nitrogen atoms (Scheme 1).

Helicenes belong to an intriguing class of polycyclic aromatic compounds that possess a characteristic helical conformation, responsible for the their commonly used name (9), as well as a collection of interesting properties, such as large circular dichroism, long triplet lifetime, absorption at low-energy wavelength, and tendency to give π - π stacking. Helicenes are indeed promising molecular species for the development of light emitting devices, sensors, and NLO-active materials. The replacement of one or more carbon atoms with nitrogens, thus forming azahelicenes, may introduce the possibility for these molecules to be involved in site-specific intermolecular interactions while maintaining their properties and their distinctive helicity. For instance, monoazahelicenes have been already shown to be able to coordinate silver cations via quinolinic and isoquinolinic nitrogen atoms positioned in the internal rim of the helicenes, affording 2:1 (helicene/ Ag^+) complexes in the solid state (10).

The 4,7,8,11-tetraazahelicene **2** (Scheme 1), having two different sets of nitrogen atoms (pyridinic/quinolinic and pyridazinic/cinnolinic), is an ideal candidate to study the site-selectivity of XB-formation in polynitrogen aromatic systems. For the same reason, **2** was selected also as a good candidate for testing computational methods as tools for predicting the site-selectivity of the XB, whenever a structural ambiguity is present. For all of these reasons the Molecular Electrostatic Potential (MEP) and Molecular Orbitals (MO) analyses of the tetraazahelicene **2** were carried out by using DFT methods in order to predict the nitrogen sites that would have been involved in the XB-formation following the co-crystallization of **2** with the 1,8-diiodoperfluorooctane derivative **1** (Scheme 1).

2. Results and Discussion

2.1 DFT Calculations

Site-selective XBs have been already reported in several cases (8, 11). The four nitrogen atoms of the tetraazahelicene **2** are all supposedly able to take part in strong XB_s. While the proton affinity (and likewise gas phase basicity) of pyridine is greater than that of any of the diazines, regarding some weaker electron-acceptors/Lewis acids (*e.g.* Li⁺, Na⁺, and K⁺), both experimental measurements and theoretical calculations show pyridine to be a considerably weaker base than pyridazine (12). This relative tendency to function as donors of electron density of different azines is consistent with other reports on their acid/base behavior and HB-acceptor ability (13). The two pyridazinic/cinnolinic nitrogen atoms on **2** were thus anticipated to function as preferred sites for the interaction with the XB-donor **1**. DFT calculations were prompted to provide more solid grounds to this hypothesis.

Deleted: -bonds.

As previously highlighted, XB possesses a marked electrostatic character, similarly to HB (14). The MEP analysis, which gives information on what molecules “see” when approaching one to the other, was thought to be extremely informative in order to ascertain the occurrence of a preferential attraction of the XB-donor **1** for either the pyridinic/quinolinic or pyridazinic/cinnolinic nitrogen atoms on **2**, prior to the establishing the actual interaction.

A plot of the MEP of **2** onto the surface of electron density with $\rho = 0.001$ a.u. is reported in Figure 1 (left). The MEP clearly indicates that the preferential sites of approaching of the iodine atoms are located on the pyridazinic/cinnolinic nitrogen atoms, around which the largest and deepest region of negative electrostatic potential (*i.e.*, red region) is present. On the other hand, smaller and less negative regions of the MEP are located on the pyridinic/quinolinic nitrogen atoms, making them less suitable to attract the incoming diiodoperfluorinated module. For comparison, in Figure 1 the MEPs of the diazahelicenes **3** (centre) and **4** (right) are also reported. Both show slightly more negative values of the electrostatic potential around, respectively, the pyridinic/quinolinic and the pyridazinic/cinnolinic nitrogen atoms, with respect to the corresponding values obtained for **2**, indicating a mutual influence between the two sets of nitrogen atoms, when fused in a single polynitrogen heterocycle (13).

Deleted: r
Deleted: r

Figure 1

Further analysis was carried out on the nature of the frontier orbitals of the tetraazahelicene **2**, in particular the Highest Occupied Molecular Orbitals (HOMOs), in order to investigate the possibility of charge-transfer interactions directing, together with the electrostatic contribution addressed above, the establishing of the XB. Such an analysis (see Figure 2) revealed that the HOMO-1 (Figure 2, centre), which is almost degenerate with the HOMO, shows both larger contributions on the nitrogen atoms of the pyridazine moiety and the appropriate symmetry to interact with the incoming iodine atoms. The first MO with similar symmetry but showing larger contributions on the pyridine nitrogen atoms is HOMO-3 (Figure 2, right), which lies in energy well below the HOMO-1. The HOMO (Figure 2, left), while being delocalized over the full molecule, has nodal surfaces in correspondence of the four nitrogen atoms and therefore cannot be responsible for such interaction. In fact, according to a previous investigation aimed at determining the best frontier MOs responsible for a given reaction (15), the analysis of the composition and shape of the last occupied molecular orbital represents precisely the best criterion to identify such MOs, which not necessarily coincide with the HOMO.

Deleted: al

As expected, the combined results given by the MEP computation, altogether with the MO analysis, firmly indicate that the pyridazinic/cinnolinic nitrogen atoms on **2** are the preferential sites for the eventual acceptance of XBs in a given supramolecular system.

Figure 2

2.2 X-Ray Diffraction Analysis

The evaporation at r.t. of a chloroform solution containing a 1:1 mixture of compounds **1** and **2** (16) yielded, after 1 day, good-quality single crystals of composition $(\mathbf{1})_3 \cdot (\mathbf{2})_2$, thus offering the opportunity for validating the prediction made by DFT calculations (see above). The single crystal X-ray diffraction analysis revealed several interesting features. As shown in the Figure 3, the observed XBs are established only with the pyridazinic/cinnolinic nitrogen atoms, as effectively predicted by the DFT calculations. Each of the two adjacent N atoms, in fact, interacts

with two different diiodoperfluoroalkane modules making the tetraazahelicene to function as a bidentate XB-acceptor. The pyridinic/quinolinic nitrogen atoms, not involved in any XB, display, instead, weak H-bond interactions (N···H-C distances of 2.61 and 2.67 Å) with adjacent tetraazahelicenes (Figure 4).

Of the two X-bonded diiodoperfluoroctane molecules, one bridges two symmetry-related tetraazahelicenes, while the second one functions as a monodentate XB-donor. Hence, the overall XB-directed assembly, indefinitely repeated over the crystal lattice, is constituted by a pentameric, zigzag shaped, $(\mathbf{1})_3 \cdot (\mathbf{2})_2$ adduct, *i.e.* two tetraazahelicenes and three diiodoperfluoroalkanes (Figure 3). Both the independent diiodoperfluoroctane molecules display the typical enantiomeric disorder of the perfluorocarbon chains, whereas only the iodine atoms engaged in XB are ordered (17).

The two observed XB_s are not equivalent. The linear bidentate XB-acceptor molecule experiences the shortest XB_s (N···I distance of 2.998 Å, while 168.3° is the mean N···I-C1(C,D) angle involving the two disordered C1C and C1D atoms), which lays on the pyridazinic/cinnolinic ring plane. Conversely, the other XB_s is significantly longer (distance 3.293 Å) with a less linear N···I-C1(A,B) angle (mean value 165.1°), consistent with a weaker XB taking place (18). This difference can be easily attributed to the vicinity of the two nitrogen atoms, which inhibits the formation of two geometrically ideal XB_s, which would have resulted in the clashing of one of the two perfluorinated modules onto the other.

Deleted: -bonds

Deleted: -bond

Deleted: -bond

Deleted: -bonds

Figure 3

The X-bonded $(\mathbf{1})_3 \cdot (\mathbf{2})_2$ pentamers are then tightly packed in the crystal lattice (no solvent molecules included) thanks to a cooperative set of various intermolecular interactions including HB, π-π stacking, and vdW and dispersion forces. In fact, besides the weak HB involving the pyridinic/quinolinic nitrogen atoms, the tetraazahelicene units are densely packed in an antiparallel fashion, showing π-π staking between the external pyridinic/quinolinic rings that maximize dipole-dipole interactions (Figure 4).

Figure 4

1
2 It is worth to be reminded that perfluorocarbon (PFC)/hydrocarbon (HC)
3 interactions are generally very weak and thus phase separation is often observed in
4 PFC/HC mixtures (19). XB is strong and specific enough to overcome this phase
5 separation to the point of triggering the self-assembly of PFCs and HCs into hybrid
6 co-crystals (20). In the system described in this paper, XB directs the self-assembly of
7 the building blocks **1** and **2** into well-defined $(\mathbf{1})_3 \cdot (\mathbf{2})_2$ pentamers. However, the
8 packing of these pentamers is strongly reminiscent of the low affinity the starting
9 materials have for each other, which results in the formation of segregated layers of
10 perfluorinated and aromatic units, as commonly observed in similar systems (Figure
11 5).

17
18 Figure 5
19
20
21
2223

3. Conclusions

24
25 In conclusion, this study shows that the tetraazahelicene **2** can be successfully used in
26 the XB-mediated assembly of supramolecular architectures. Indeed, the self-assembly
27 of the 1,8-diiodoperfluorooctane **1** with the tetraazahelicene **2** produced a lattice of
28 packed pentameric units $(\mathbf{1})_3 \cdot (\mathbf{2})_2$, the monomers of which are connected by two non-
29 equivalent XB_s. Interestingly, only the pyridazinic/cinnolinic nitrogen atoms were
30 involved in the formation of XB_s with the 1,8-diiodoperfluorooctane **1**, resulting in a
31 site-selective supramolecular synthesis mediated by XB. This selectivity parallels the
32 relative HB basicity of the competing pyridinic/quinolinic and pyridazinic/cinnolinic
33 nitrogen sites towards weaker Lewis acids. In this respect, XB shows the same
34 selectivity found for HB in related polynitrogen heteroaromatics (12, 13).
35
3637
38
39
40
41
42
43
44
45
46
47
48
49
50
51
52
53
54
55
56
57
58
59
60

Deleted: -bonds.

Deleted: -bonds

In the described pentameric system $(\mathbf{1})_3 \cdot (\mathbf{2})_2$, the self-sorting process mediated by XB favours the modules' binding sites which allows for an optimal phase segregation between perfluorocarbon and hydrocarbon domains on the basis of thermodynamic considerations.

Little is known on how to predict and control selectivity among different supramolecular synthons. In the case reported in this article, DFT calculations were able to predict the observed site-selectivity based on the analysis of both the electrostatic potential and the nature of the HOMOs of the tetraazahelicene **2**. These theoretical data suggest a twofold control, by electrostatic and charge-transfer

1
2 interactions, on the establishing of XB in this system, which selected the
3 pyridazinic/cinnolinic atoms, over the pyridinic/quinolinic nitrogen atoms, as
4 preferred sites for the XB formation with **1**. Such DFT approach has a general validity
5 and, therefore, can be applied whenever the site-selectivity of the XB in polynitrogen
6 systems is of concern.
7
8

Deleted: -bond

9
10 The results described in this article demonstrates that the tetraazahelicene **2**
11 might be used as a new tecton in supramolecular chemistry capable of being involved
12 into a two-fold set of intermolecular interactions showing an orthogonal selectivity
13 towards the two different set of nitrogen atoms present onto **2**. Self-assembly
14 processes using the tetraazahelicene **2** and based on simultaneous XB and HB, or XB
15 and metal coordination, are currently in progress.
16
17
18

19
20
21
22 **4. Experimental Section**

23 **4.1 Synthesis**

24
25 The synthesis of the tetraazahelicene **2** is an optimized version of the procedure
26 reported by R. Huisgen in *Justus Liebigs Annalen der Chemie* **1948**, 559, 101-152.
27 Compound **2**: ^1H NMR (250MHz, CDCl₃): δ 9.11 (2H, dd, J₁=1.5Hz, J₂= 4.2 Hz), δ
28 9.00 (2H, d, J=8.75 Hz), δ 8.84 (2H, d, J=9.25Hz), δ 8.50 (2H, d, J=9 Hz), δ 7.42 (2H,
29 m); ^{13}C NMR(63MHz): δ 152.62, 149.74, 146.04, 136.07, 132.71, 130.80, 123.17,
30 120.12, 119.25; ESI Mass: calc. for C₁₈H₁₀N₄ 282, found 283 [M+H]⁺.
31
32
33
34

35
36 **4.2 Crystal growth and X-ray diffraction**

37 Single crystals were obtained by dissolving at room temperature equimolar amounts
38 of the 1,8-diiodoperfluorooctane **1** and the tetraazahelicene **2** in a vial of clear
39 borosilicate glass, using chloroform as solvent. The open vial was introduced in a
40 closed cylindrical glass jar containing paraffine oil. Chloroform was allowed to
41 diffuse at room temperature and after one day the formation of orange crystals was
42 observed.
43
44

45
46 **4.2.1 Complex (1)₃·(2)₂**

47
48 MF = C₆₀H₂₀F₄₈I₆N₈, FW = 2526.24, triclinic, space group P-1, a = 9.897(2), b =
49
50 10.763(2), c = 20.010(3) Å, α = 96.23(2), β = 90.90(2), γ = 116.07(2), V = 1898.5(6)
51
52

Deleted: orthorhombic

1
2 Å³, Z = 1, D_x = 2.210 Mg·m⁻³, μ (Mo-K α) = 2.618 mm⁻¹; crystal dimensions
3 0.44x0.26x0.23 mm³, λ = 0.71073 Å (Mo-K α radiation), graphite monochromator,
4 Bruker SMART-APEX CCD diffractometer. Data collection: ω and φ scan mode, 2 θ
5 < 50°; 10790 collected reflections, 10790 unique [6736 with $I_o > 2\sigma(I_o)$], merging R =
6 0.02530. The structure was solved by *SIR2002* (21) and refined by *SHELXL* (22), full-
7 matrix least-squares based on F_o^2 , with weights w = 1/[$\sigma^2(F_o)^2 + (0.0847P)^2$], where P
8 = ($F_o^2 + 2F_c^2$)/3. H atoms were in calculated positions. The final consistency index
9 were R = 0.0667 and R_w = 0.1488 [0.0471 and 0.1403 respectively for $I_o > 2\sigma(I_o)$],
10 goodness-of-fit = 1.029. The final map ranges between -0.83 and 0.81 e·Å⁻³. Detailed
11 crystallographic data were deposited as CCDC 783798 with the Cambridge
12 Crystallographic Data Centre, 12 Union Road, Cambridge CB2 1EZ, UK and can be
13 obtained free of charge from <http://www.ccdc.cam.ac.uk/products/csd/request/>.
14
15

21 22 23 4.3 Computational details

24 Geometry optimizations of the di- and tetraazahelices were carried out in the gas
25 phase with the Gaussian '03 software package (23) at DFT (B3LYP) level (24), using
26 the 6-311++G** basis set for all atoms. The basis set for iodine (25) was downloaded
27 from the Basis Set Exchange site (26).
28
29

34 Acknowledgements

35 This work was funded by Fondazione Cariplo ("New-Generation Fluorinated
36 Materials as Smart Reporter Agents in ¹⁹F MRI") and MIUR ("Engineering of the
37 Self-assembly of Molecular Functional Materials via Fluorous Interactions").
38
39

Captions for the on-line publication with figures in colours

Scheme 1. Molecular formulae of the XB-donor **1** and acceptors **2-4** mentioned in the text. Pyridinic/quinolinic nitrogen atoms are reported in blue, while the pyridazinic/cinnolinic ones are in red.

Figure 1. Plots of the B3LYP/6-311++G** electrostatic potential of the compounds **2** (left), **3** (centre), and **4** (right) mapped on the respective isosurfaces (0.001 a.u.) of electron density. Minimum values of electrostatic potential are -0.0593 and -0.0447 a.u. (on the pyridazinic/cinnolinic and pyridinic/quinolinic nitrogen atoms, respectively, of **2**), -0.0527 a.u. (**3**), and -0.0655 a.u. (**4**).

▼
Figure 2. Surface plot of the B3LYP/6-311++G** HOMO (left), HOMO-1 (centre) and HOMO-3 (right) of the tetraazahelicene **2** (isovalue=0.02 a.u.).

Deleted: Figure 1. Plots of the B3LYP/6-311++G** electrostatic potential of the compounds **2** (left), **3** (centre), and **4** (right) mapped on the respective isosurfaces (0.001 a.u.) of electron density.¶

Figure 3. Spacefill representation of the XB-assembled pentamer (**1**)₃·(**2**)₂ in the crystal (colour code: white: H; gray: C; blue: N; violet: I; yellow: F).

Figure 4. HB and π-π stacking motifs observed in the crystal structure (the second H-bonded layer of molecules of **2** is shown in red).

Figure 5. Representation of the segregation into layers in the lattice of the molecular components **1** (spacefill) and **2** (capped sticks).

Captions for the printed version with figures in B/W

Scheme 1. Molecular formulae of the XB-donor **1** and acceptors **2-4** mentioned in the text.

Figure 1. Plots of the B3LYP/6-311++G** electrostatic potential of the compounds **2** (left), **3** (centre), and **4** (right) mapped on the respective isosurfaces (0.001 a.u.) of electron density. Minimum values of electrostatic potential are -0.0593 and -0.0447 a.u. (on the pyridazinic/cinnolinic and pyridinic/quinolinic nitrogen atoms, respectively, of **2**), -0.0527 a.u. (**3**), and -0.0655 a.u. (**4**).

Figure 2. Surface plot of the B3LYP/6-311++G** HOMO (left), HOMO-1 (centre) and HOMO-3 (right) of the tetraazahelicene **2** (isovalue=0.02 a.u.).

Figure 3. Spacefill representation of the XB-assembled pentamer (**1**)₃·(**2**)₂ in the crystal.

Figure 4. HB and π-π stacking motifs observed in the crystal structure (the second H-bonded layer of molecules of **2** is shown in black).

Figure 5. Representation of the segregation into layers in the lattice of the molecular components **1** (spacefill) and **2** (capped sticks).

- M. D. *Science* **2006**, *314*, 1437; Verbiest, T.; Van Elsocht, S.; Kauranen, M.; Hellemans, L.; Snaauwaert, J.; Nuckolls, C.; Katz, T. J.; Persoons, A. *Science* **1998**, *282*, 913; Verbiest, T.; Sioncke, S.; Persoons, A.; Vylicky, L.; Katz, T. J. *Angew. Chem., Int. Ed.* **2002**, *41*, 3882; Furche, F.; Ahlrichs, R.; Wacksmann, C.; Weber, E.; Sobanski, A.; Vögtle, F.; Grimme, S. *J. Am. Chem. Soc.* **2000**, *122*, 1717; Autschbach, J.; Ziegler, T.; van Gisbergen, S. J. A.; Baerends, E. J. *J. Chem. Phys.* **2002**, *116*, 6930; Spassova, M.; Asselberghs, I.; Verbiest, T.; Clays, K.; Botek, E.; Champagne, B. *Chem. Phys. Lett.* **2007**, *439*, 213; Champagne, B.; André, J. M.; Botek, E.; Licandro, E.; Maiorana, S.; Bossi, A.; Clays, K.; Persoons, A. *Chem. Phys. Chem.* **2005**, *5*, 1438.
- (10) Misek, J.; Teply, F.; Stara, I.G.; Tichy, M.; Saman, D.; Cisarova, I.; Vojtisek, P.; Stary I.; *Angew. Chem. Int. Ed.* **2008**, *47*, 3188-3191.
- (11) Bruce, D. W.; Metrangolo, P.; Meyer, F.; Pilati, T.; Präsang, C.; Resnati, G.; Terraneo, G.; Wainwright, S. G.; Whitwood, A. C.; *Chem. Eur. J.* **2010**, DOI: 10.1002/chem.201000717; Lapadula, G.; Judas, N.; Frisčić, T.; Jones, W.; *Chem. Eur. J.* **2010**, *16*, 7400-7403; Metrangolo, P.; Meyer, F.; Pilati, T.; Proserpio, D. M.; Resnati, G.; *Chem. Eur. J.* **2007**, *13*, 5765-5772; Metrangolo, P.; Präsang, C.; Resnati, G.; Liantonio, R.; Whitwood, A. C.; Bruce, D. W.; *Chem. Commun.* **2006**, 3290-3292; Syssa-Magalé, J.-L.; Boubekeur, K.; Palvadeau, P.; Meerschaut, A.; Schöllhorn, B.; *CrystEngComm* **2005**, 302-308; Syssa-Magalé, J.-L.; Boubekeur, K.; Schöllhorn, B.; *J. Mol. Struct.* **2005**, *737*, 103-107; Amico, V.; Meille, S. V.; Corradi, E.; Messina, M. T.; Resnati, G.; *J. Am. Chem. Soc.* **1998**, *120*, 8261-8262.
- (12) Lipkind, D.; Chickos, J. S.; Liebman, J. F.; *Struct. Chem.* **2009**, *20*, 617-618.
- (13) Berthelot, M.; Laurence, C.; Safar, M.; Besseau, F.; *J. Chem. Soc., Perkin Trans. 2* **1998**, 283-290; Tabatchnik, A.; Blot, V.; Pipelier, M.; Dubreuil, D.; Renault, E.; Le Questel, J.-Y.; *J. Phys. Chem. A* **2010**, *114*, 6413-6422.
- (14) Bianchi, R.; Forni, A.; Pilati, T. *Chem. Eur. J.* **2003**, *9*, 1631-1638; Bianchi, R.; Forni, A.; Pilati, T. *Acta Crystallogr. Sect. B* **2004**, *60*, 559-568; Forni, A. *J. Chem. Phys. A* **2009**, *113*, 3403-3412.
- (15) Da Silva, R. R.; Ramalho, T. C.; Santos, J. M.; Figueroa-Villar, J. D.; *J. Phys. Chem. A* **2006**, *110*, 1031-1040 and references cited therein.
- (16) The full characterization of the molecular and supramolecular species reported in this article is given in the experimental part and in the supporting information.
- (17) Dey, A.; Metrangolo, P.; Pilati, T.; Resnati, G.; Terraneo, G.; Wlassics, I.; *J. Fluorine Chem.* **2009**, *130*, 816-823.
- (18) The sum of the VdW radii for N (155 pm) and I (198 pm) is 353 pm. See Bondi, A.; *J. Phys. Chem.* **1964**, *68*, 441-451.
- (19) Smart, B. E.; *J. Fluorine Chem.* **2001**, *109*, 3-11.
- (20) Metrangolo, P.; Pilati, T.; Resnati, G.; Stevanazzi, A.; *Curr. Opin. Colloid Interface Sci.* **2003**, *8*, 215-222.
- (21) Burla, M. C.; Camalli, M.; Carrozzini, B.; Casciarano, G. L.; Giacovazzo, C.; Polidori, G.; Spagna, R.; *J. Appl. Cryst.* **2003**, *36*, 1103.
- (22) Sheldrick, G. M.; *Acta Cryst.* **2008**, *A64*, 112-122.
- (23) Gaussian 03, Revision C.02, Frisch, M. J.; Trucks, G. W.; Schlegel, H. B.; Scuseria, G. E.; Robb, M. A.; Cheeseman, J. R.; Montgomery, Jr., J. A.; Vreven, T.; Kudin, K. N.; Burant, J. C.; Millam, J. M.; Iyengar, S. S.; Tomasi, J.; Barone, V.; Mennucci, B.; Cossi, M.; Scalmani, G.; Rega, N.; Petersson, G. A.; Nakatsuji, H.; Hada, M.; Ehara, M.; Toyota, K.; Fukuda, R.; Hasegawa, J.; Ishida, M.; Nakajima, T.; Honda, Y.; Kitao, O.; Nakai, H.; Klene, M.; Li, X.; Knox, J. E.; Hratchian, H. P.; Cross, J. B.; Bakken, V.; Adamo, C.; Jaramillo, J.; Gomperts, R.; Stratmann, R. E.; Yazyev, O.; Austin, A. J.; Cammi, R.; Pomelli, C.; Ochterski, J. W.; Ayala, P. Y.; Morokuma, K.; Voth, G. A.; Salvador, P.; Dannenberg, J. J.; Zakrzewski, V. G.; Dapprich, S.; Daniels, A. D.; Strain, M. C.; Farkas, O.; Malick, D. K.; Rabuck, A. D.; Raghavachari, K.; Foresman, J. B.; Ortiz, J. V.; Cui, Q.; Baboul, A. G.; Clifford, S.; Cioslowski, J.; Stefanov, B. B.; Liu, G.; Liashenko, A.; Piskorz, P.; Komaromi, I.; Martin, R. L.; Fox, D. J.; Keith, T.; Al-Laham, M. A.; Peng, C. Y.; Nanayakkara, A.; Challacombe, M.; Gill, P. M. W.; Johnson, B.; Chen, W.; Wong, M. W.; Gonzalez, C.; and Pople, J. A.; Gaussian, Inc., Wallingford CT, **2004**.
- (24) Becke, A. D.; *J. Chem. Phys.* **1993**, *98*, 5648-5652; Lee, C.; Yang, W.; Parr, R. G.; *Phys. Rev. B: Condens. Matter* **1988**, *37*, 785-789.
- (25) Glukhovstev, M. N.; Pross, A.; McGrath, M. P.; Radom, L.; *J. Chem. Phys.* **1995**, *103*, 1878-1885.
- (26) Feller, D.; *J. Comp. Chem.* **1996**, *17*, 1571-1586; Schuchardt, K. L.; Didier, B. T.; Elsethagen, T.; Sun, L.; Gurumoorthi, V.; Chase, J.; Li, J.; Windus, T. L.; *J. Chem. Inf. Model.* **2007**, *47*, 1045-1052.